JOURNAL OF MATERIALS SCIENCE **32** (1997) 3277–3282

Hydrogen plasma transport and deposition of films from a solid boron source

J. S. CROSS*, S. KOMATSU†, J. TANAKA, M. MIENO, Y. SUETSUGU,
J. SAKAGUCHI, Y. MORIYOSHI‡
National Institute for Research in Inorganic Materials, 1-1 Namiki, Tsukuba, Ibaraki 305 Japan

W. R. STEPHENSON
Department of Statistics, Snedecor Hall, Iowa State University, Ames, IA 50011 USA

Thin boron films were produced on Si substrates from a solid boron source and a hydrogen plasma. The plasma was generated using a 13.56 MHz generator and films were deposited with a forward radio frequency (RF) power of 2.0 kW. At pressures from 0.931–2.26×10^2 Pa under high hydrogen concentrations a capacitively coupled plasma (CCP) was observed whereas at low hydrogen concentrations an inductively coupled plasma (ICP) was observed. The films were predominantly deposited with an ICP but in one case a film was deposited using a CCP discharge. The deposited films consisted primarily of boron, but they also contained oxygen and silicon. The films were amorphous at 225 and 350 °C, but revealed X-ray diffractions at 475 °C. It was concluded that the hydrogen concentration, RF plasma power and surface temperature as well as the plasma-boron source interactions strongly influenced the film thickness and composition.

1. Introduction

Boron films are of interest for use in ultraviolet mirrors [1] and when combined with oxygen or nitrogen as superhard materials. Typically, chemical vapour deposited (CVD) boron containing films are produced from volatile B_2H_6 or BCl_3 gas precursors which are extremely toxic. These gaseous precursors require the use of an expensive gas handling system for the operator's safety. An alternative to this is to produce the precursor within the chamber using a hydrogen plasma and a solid boron source [2]. With the hydrogen plasma transport system the boron precursor is generated in low concentrations within the system, thus eliminating the need for an expensive gas handling system.

In 1985, this process was demonstrated in the synthesis of boron films on Si substrates [2]. However, since this initial study little research has been done using this process. It was the objective of this study to re-examine this process in more detail. Specially, we were not only interested in examining how the process parameters effected the film deposition but also the effect the plasma has on the boron source.

2. Experimental methods

Films were deposited on Si (1 0 0) $18 \times 18 \times 0.5$ mm substrates cut from a 100 mm Si wafer. The substrates were cleaned in an ultrasonic bath with acetone. Si substrates were loaded on to a BN holder which was heated radiatively by W wire powered by a d.c. power supply. The substrate temperature was measured by a thermocouple which was connected to a temperature controller.

The deposition chamber consisted of stainless steel and quartz. The boron source consisted of B pieces placed inside a BN crucible which sat inside a quartz tube (6 cm inside diameter by 10 cm long) (Fig. 1). The outside of the quartz tube was cooled by cooling water. A three turn water-cooled copper coil surrounded the tube and was connected to a 5 kW 13.56 MHz radio frequency (RF) generator. Less than 3% of the forward RF power was reflected. A throttling valve was used to control the system pressure which was measured using a capacitance manometer.

Depositions were conducted over a range of conditions with a total gas flow rate of 100 s.c.c.m. The gases, ultra pure H_2 and He, were controlled by mass flow controllers. The H_2 flow rates examined were 0, 10, 50, 90 and 100 s.c.c.m. Initially, the RF power was varied from 0.5 kW to 2.6 kW, but the film deposition results presented in this study were conducted with the RF power fixed at 2.0 kW. The deposition pressure was set at values of 0.93, 1.59, 1.2 or 2.26×10^2 Pa and substrate temperatures of 225, 350 or 475 °C.

Present addresses: * Fujitsu Laboratories, 10-1 Morinosato-wakamiya, Atsugi, 243-01 Japan; ‡ Department of Materials Science, Hosei University, Koganeishi, Tokyo, Japan.
† Author to whom correspondence should be addressed.

0022–2461 © *1997 Chapman & Hall*

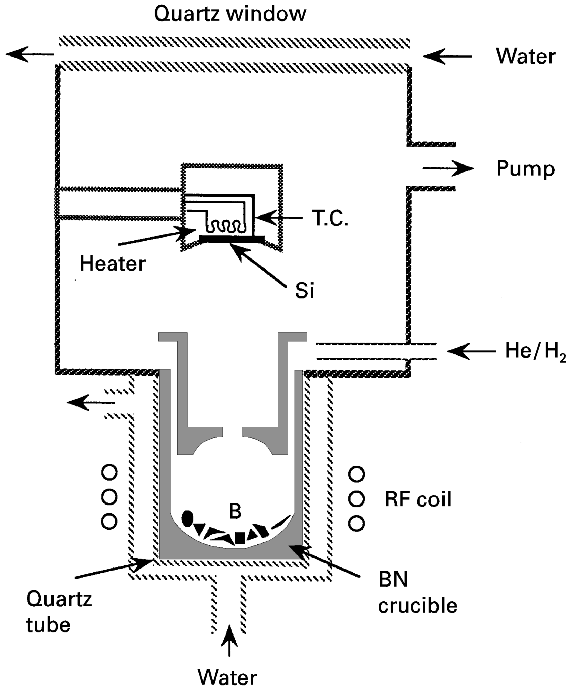

Figure 1 Hydrogen plasma transport and deposition reactor with solid boron source (B).

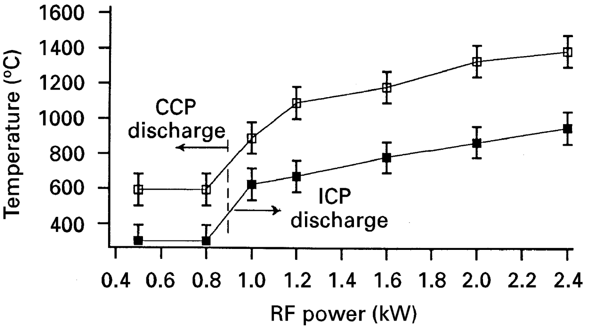

Figure 2 B source (□) and BN crucible (■) temperatures as a function of RF power with a 10 s.c.c.m. H_2 flow rate, 90 s.c.c.m. He flow rate and pressure of 0.931×10^2 Pa. Note: the BN crucible temperatures at 0.5 and 0.8 kW are estimations.

Before each deposition the chamber was cleaned with water, acetone and ethanol, respectively, in order to remove any residue from previous depositions. For each deposition approximately, 3.5 g of boron metal (3–5 mm pieces, 99.9%) as received was loaded into the BN crucible. The chamber was evacuated using a diffusion pump and a LN_2 trap. After three hours the chamber obtained a minimum pressure of 1.33×10^{-3} Pa as measured by an ionization gauge (Ulvac). During the depositions He and H_2 gases flowed into the chamber and were evacuated by a rotary pump fitted with a LN_2 foreline trap.

At the beginning of each deposition the temperature controller ramped the Si substrate up to the desired temperature in 15 min. To initiate the discharge the plasma was ignited on only He gas at a RF power of 0.5 kW for 5 min. The boron was initially at room temperature, but after 5 min in the He plasma the boron heated up to approximately 600 °C. The H_2 gas was then admitted into the chamber and the deposition was started. The conditions were then set for those specified for the deposition where they remained for one hour.

Two process responses were recorded for each set of experimental conditions: boron source temperature and film thickness. The film thickness was measured using a Dektak profilometer. The boron metal temperature was recorded using a Minolta pyrometer, IR-630, wavelengths from 0.8–1.1 μm with an arbitrarily chosen emissivity of 0.7 for the boron source and BN crucible. (The pyrometer accurately measured temperatures above 600 °C.)

The temperature of the boron source was not measured during the deposition experiment because the substrate holder interfered with the pyrometer temperature measurements (Fig. 1). A separate series of experiments were conducted with a blank flange in place of the substrate holder in order to record the boron source temperature. The boron source temperature was measured by focusing the pyrometer through the quartz window on the B source and recording the temperature at each combination of pressure and H_2 concentrations used in the depositions. The BN crucible temperature was also recorded by focusing the pyrometer on the BN crucible exterior as measured through the quartz tube and in between the RF induction coil.

Characterization of the deposits was conducted using X-ray diffraction (XRD) and scanning electron microscopy (SEM, Fourier transform infra-red (FTIR), X-ray photoelectron (XPS), secondary ion mass (SIMS) and Auger electron spectroscopies (AES). The samples analysed by AES were gold coated (20 nm thick) prior to analysis.

3. Results

3.1. CCP and ICP discharges

We investigated the relationship between the B source and BN crucible temperature as a function of the forward RF power while the H_2 gas flow rate and pressure were held constant (Fig. 2). The plasma that developed was confined primarily to the BN crucible however, a weaker discharge was also observed in the deposition chamber. At approximately 0.9 kW, there was a transition in the plasma and an increase in the boron source and BN crucible temperatures (Fig. 2). This transition was also visibly observable with a noted increase in the plasma intensity or brightness. The plasma that formed at low power is known as a capacitively coupled plasma (CCP) or e-discharge and at high power an inductively coupled plasma (ICP) or h-discharge [3]. This same phenomena has also been observed in other reactor systems [4].

In Fig. 2 the transition occurred at 0.9 kW with a H_2 gas concentration of 10% and pressure of 0.93×10^2 Pa. However, with higher H_2 concentrations the transition did not occur below 2.0 kW. As discussed below, this transition has an effect on the film deposition (Table I).

TABLE I Summary of film deposition results with a forward RF power of 2.0 kW.

Run	Temperature Si (°C)	Process variables ($\times 10^2$ Pa)		Responses	
		Press.	H_2 (s.c.c.m.)	Temperature B (°C)	Thickness (nm)
1	225.0	0.931	10.0	1510^i	110
2	475.0	0.931	10.0	1510^i	no
3	225.0	0.931	90.0	1540^i	215
4	475.0	0.931	90.0	1540^i	78
5	225.0	2.261	10.0	1420^i	429
6	475.0	2.261	10.0	1420^i	379
7	225.0	2.261	90.0	620^c	no
8	475.0	2.261	90.0	620^c	no
9	350.0	1.596	50.0	1300^i	75
10	350.0	1.596	50.0	1300^i	50
11	350.0	1.596	100.0	630^c	406
12	350.0	1.596	0.0	1450^i	no

Note: ^{i}represents inductively coupled plasma and ^{c}represents capacitively coupled plasma discharge. Also, no indicates that no film of measurable thickness film was deposited, except in one case for run 8 where no film was measurable by the profilometer but the substrate surface appeared to be covered by a very thin layer.

3.2. Films

Films were deposited over a range of hydrogen concentrations, pressures and temperatures, as shown in Table I. In several cases no films of measurable thicknesses were deposited. However, when films were deposited the thicknesses ranged from 50 to 429 nm (Table I). A typical cross-sectional view of a film deposited at 225 °C revealed little film texture (Fig. 3).

An Auger differentiated spectrum recorded after a 40 s Ar^+ etch revealed that the film contained measurable amounts of B, O and Si, but little C (Fig. 4). As shown in Fig. 4, both elemental Si (92 eV) and Si from SiO_2 (76 eV) were detected in the differentiated AES spectrum [5].

AES depth profiles showed measurable amounts of B, O and Si in the film. The B/O atomic ratio in the film deposited at 225 °C was dependent on the location of the analysis on the Si substrate (Fig. 5a and b). Analysis of the film indicated that a boron-rich region existed near the centre (Fig. 5a) and an oxygen-rich region near the edge (Fig. 5b). Further Auger analysis in the boron-rich region of the films deposited at 350 and 475 °C had similar B/O atomic ratios of 8 to 1 (runs 10 and 6), as observed in Fig. 5a.

XPS analysis of the film B1s binding energy spectrum appeared to be composed of three different Gaussian curves (Fig. 6). The Gaussian maxima were assigned to B–B (187.5 eV), B–H (188.0 eV) and B–O (193.0 eV) bonds [6]. These three bands existed both in the film (Fig. 6) as well as in the as received boron source material (Fig. 7), although the 193 eV band was stronger in the film than in the source. The spectrum recorded on the film surface before and after etching were similar. However, after Ar ion etching the peaks slightly broadened.

Films deposited at 475 °C and analysed by XRD showed preferred orientation with diffractions at 0.318 and 0.158 nm. These diffractions resemble those of both cubic-B_2O_3 planes of (3 1 0) at 0.321 nm and (6 2 0) at 0.16 nm, and boric acid (H_2BO_3) at 0.318 (0 0 2) and 0.16 nm (0 0 4), respectively [7]. Films deposited at 350 and 225 °C were without strong diffractions except for Si at 0.136 nm.

FTIR data of the films showed strong bands at 3110, 2255, 1368, 1183 and 839 wavenumbers (cm^{-1})

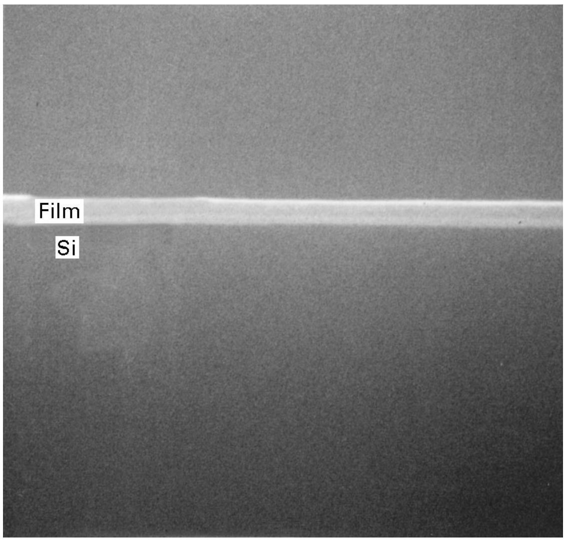

Figure 3 SEM micrograph of film deposited at 225 °C (run 1).

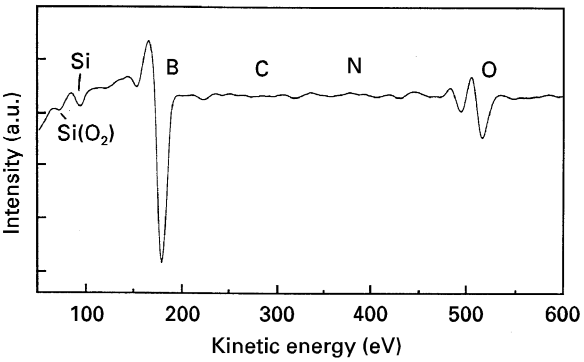

Figure 4 Auger differential spectrum for a film deposited at 225 °C, after the film was etched for 40 s with Ar^+ (run 1).

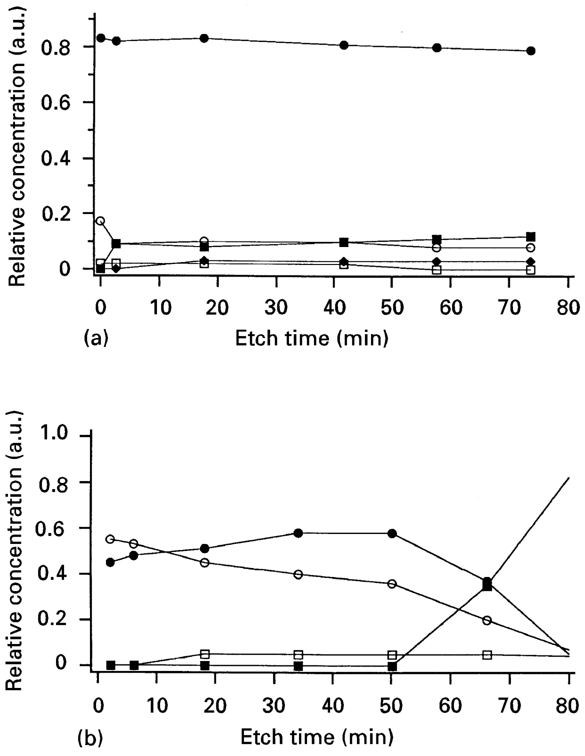

Figure 5 Auger depth profiles of films deposited at 225 °C, measurements were made near the (a) centre and (b) perimeter (run 1). (●) B; (○) O; (■) Si; (◆) N; (□) SiO_2.

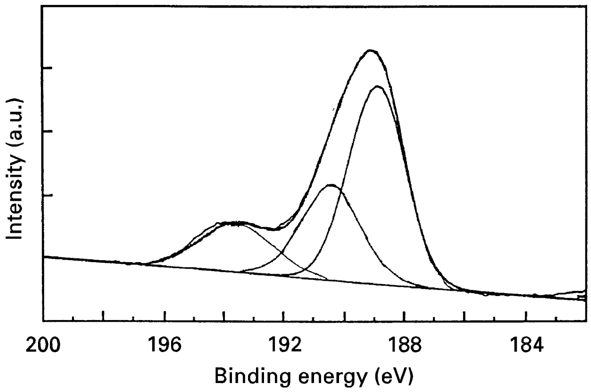

Figure 6 XPS spectrum of film deposited at 475 °C (run 6).

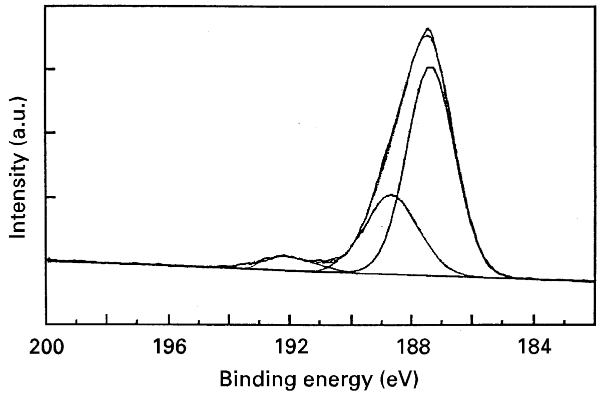

Figure 7 XPS spectrum of the as-received boron source.

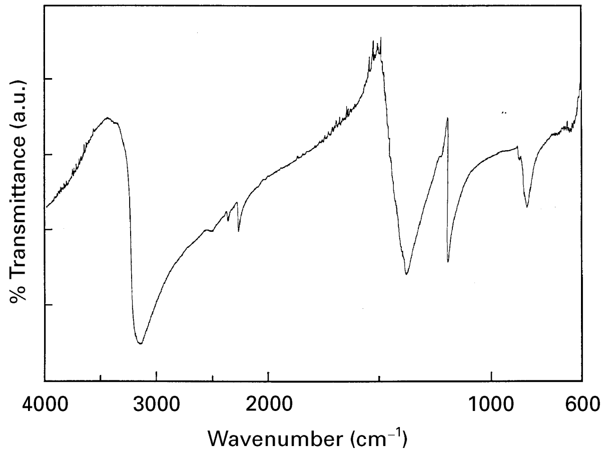

Figure 8 FTIR spectrum of film deposited at 475 °C (run 6).

TABLE II Calculated thermodynamic equilibrium condensed phase compositions of H, B, He and O system at a constant pressure of 1.33 × 10^2 Pa.

Temperature (°C)	Molar ratio O:B = 2:1	Molar ratio O:B = 1:1
27.0	HBO_2 (100)	B (50), B_2O_3 (50)
127–450	B_2O_3 (100)	B (50), B_2O_3 (50)
460–1227	$B_2O_3[l]$ (100)	B (50), $B_2O_3[l]$ (50)

The values in parenthesis are in molar percentages. The compounds are solids except as indicated by *l* for a liquid.

(Fig. 8). These bands correspond to O–H stretching (3110), B–H vibration (2255), B–O stretching (1368) B–O–H bending (1183) and B–O stretching (839) [2, 8].

Although the plasma process is not a thermodynamic equilibrium process, thermodynamic calculations give an indication of the stability of the material that is expected from a given set of reactants under thermodynamic equilibrium. The calculations were made on the H, B, O and He system using a computer program, Solgasmix-PV [9, 10]. The program calculated the equilibrium composition by minimization of the system Gibbs free energy and conservation of mass.

Equilibrium calculations were made at two different B to O molar ratios with excess hydrogen at a constant pressure of 1.33 × 10^2 Pa. The calculations showed that with a B to O ratio of 1.0 to 1.0, both B and B_2O_3 coexist in the solid phase at 27 °C (Table II). This composition is stable up to 450 °C. Above 460 °C until the boiling point of B_2O_3 at 1227 °C, both solid B and liquid B_2O_3 exist as condensed phases. If the oxygen ratio is doubled, the most stable phase formed at 27 °C is a boric acid, HBO_2 (Table II). The boric acid is not stable at 127 °C, where equilibrium indicated that only solid boric oxide, B_2O_3, exists. The solid B_2O_3 remained up to 450 °C, and at 460 °C the B_2O_3(s) melts to form a liquid (Table II). Above 460 °C no solid phase is thermodynamically stable at this B to O ratio.

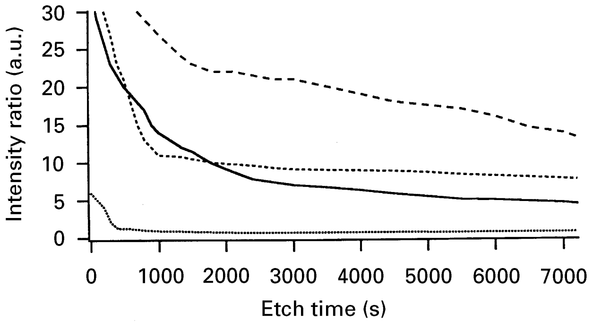

Figure 9 SIMS depth profiles of selected negative a.m.u. ion ratios of the as-received boron source (starting material-SM) and after deposition (AD) in which the boron source was exposed to H_2/He plasma discharge and temperature of 1300 °C (run 10). (—) $16^-/11^-$; (....) $12^-/11^-$; (- - -) $16^-/11^-$; (— — —) $12^-/11^-$.

3.3. Boron source

The temperatures of the boron source were also measured in a separate set of experiments but using the same deposition conditions. The results of the temperature measurements are listed in Table I along with the film deposition results. The boron source temperature ranged from 620 to 1540 °C, depending upon the hydrogen concentration and pressure. By analogy then, films were deposited with source temperatures of approximately 630 °C for run 12 and in excess of 1500 °C for several different runs (Table I). The relationship between the source temperature and film thickness will be further discussed in Section 4.

The boron source was also analysed by XPS and SIMS. XPS showed that the as-received B source had bands matching those B and B_2O_3 (Fig. 7). A SIMS depth profile analysis was conducted on the B source starting material (SM) and after the deposition (AD) for run 10. The intensity of the negative ion mass to charge ratios were collected for a.m.u. 11, 12 and 16 which corresponds to B, C and B–H and O, respectively. Analysis of the as-received boron showed the $16^-/11^-$ and $12^-/11^-$ ratios were highest at the surface and decreased in intensity during the depth profile (Fig. 9). In this case $16^-/11^-$ ratio was much larger than the $12^-/11^-$ ratio. A dynamic SIMS depth profile of the boron source after the deposition showed a high $12^-/11^-$ ratio near the surface (Fig. 9) which gradually decreased in intensity as the material was bombarded with Cs^+. The $16^-/11^-$ ratio was much lower after the deposition compared with the as-received material.

4. Discussion

In most depositions an ICP discharge formed and led to film deposition (Table I). This is in agreement with previous results which showed that when the boron source was exposed to an ICP discharge boranes were detectable in mass spectroscopy and films were deposited [2]. However, in several runs nos 2 and 12, even though a ICP discharge formed, no measurable film was deposited. We also observed in run 11, with an inlet gas of 100% H_2, that a film was deposited from a CCP discharge. Conversely, in run 12, the inlet gas consisted of 100% He which resulted in no film deposition. Thus, It appears that having H_2 in the gas stream is necessary, but not sufficient to deposit a film as evident by runs 2, 7 and 8. Secondly, it is possible to deposit films using both the ICP discharge and CCP discharge although under limited conditions.

4.1. Substrate temperature

The temperature of the substrate also appears to influence the film thickness, as noted in runs 1 and 2, as well as in runs 3 and 4. At 475 °C in runs 2 and 4 little or no film is deposited but if the substrate temperature is lowered the film deposition thickness increases, as in runs 1 and 3. However, as noted in runs 7 and 8, in both cases a film was not deposited at either temperature (Table I).

In this reactor the Si substrate was heated radiatively by a W wire on the back side. It was expected that there were radial temperature distributions on the Si surface based upon heat conduction equations but they were thought to be insignificant. These distributions would lead to a temperature maximum near the substrate centre and minimum near the edge. The boric acid and oxides have higher vapour pressures than does boron metal under these deposition conditions, so it is proposed that these oxygen-rich materials are depositing more selectively near the edge because of the lower temperature. This results in a boron-rich region near the centre and an oxygen-rich region near the edge, because of temperature variations on the Si surface. This also explains why B and O species were detected by AES and B–H, B–O and B–B bonding was measured by XPS with B–O and B–H bonding confirmed by FTIR spectroscopy (Figs 4, 5, 6 and 8). We expect that the O–H signal observed in the films by FTIR is due to the film decomposition into boric acid by exposure to water vapour in air. This was also observed previously [2].

4.2. SIMS analysis

SIMS analysis of the boron source showed a boron oxide overlayer on the starting material and on the source after the deposition, as evident by the a.m.u. $16^-/11^-$ signal (Fig. 9). The formation of the oxide on the surface results from the fact that B is thermodynamically unstable in atmosphere and readily forms boron oxides or boric acid. (Both the films and B source were stored in air.) The $12^-/11^-$ signal ratio for the as received material was high at the surface but then gradually decreased to a steady state value of approximately 0.7. The a.m.u. 12^- signal consisted of both carbon and B–H species because the mass separation slits on the SIMS spectrometer were in the fully open position during the analysis. After the deposition, the a.m.u. $12^-/11^-$ ratio significantly increased as a result of its exposure to the H_2 plasma with a steady state value of approximately 14 (Fig. 9). We feel that the twenty-fold increase in the a.m.u. $12^-/11^-$ signal ratio after the deposition is primarily due to presence of B–H on the B source surface because the deposition system contained a LN_2 trap on both the diffusion pump and roughing pump to reduce the back-streaming of hydrocarbons and C was not detected by AES in the films. The significant increase in the a.m.u. 12^- signal indicates that the B source was hydrogenated by the hydrogen plasma and that hydrogen may have diffused into the bulk of the B source. Considering these SIMS results of the B source, then it appears that further reaction with hydrogen produces gaseous boranes which were detected by mass spectroscopy in the previous study [2].

4.3. Reactor design and impurities

In this system there were several sources of oxygen in the films, including B_2O_3 on the B source surface, background water vapour in the chamber, and oxygen from quartz in the deposition chamber. In this study exposure of the quartz tube, although limited by the BN crucible, may have contributed to the incorporation of Si and SiO_2 into the film, as measured by AES (Fig. 4). This type of reactor which is designed to create a high density plasma in the quartz chamber can also be used for etching Si [4]. Therefore, proper shielding as well as water cooling are required for solid materials or surfaces exposed to the plasma [4].

In a separate study where boron films were produced by e-beam evaporation, oxygen was also incorporated into boron films if the system background pressure was greater than 1.33×10^{-4} Pa [8]. In this system the minimum background pressure was 1.33×10^{-3} Pa; so it is likely that oxygen from water vapour was dissociating in the plasma and being incorporated into the films.

Thermodynamic calculations showed that if oxygen were present in the system thermodynamically it would be incorporated into the film (Table II) when the deposition temperature was below 450 °C. In Table II we observed that in two out of the four experiments at 475 °C films were deposited above 450 °C. This indicates that under certain combinations of pressure and hydrogen gas concentrations the effect of impurities in the system was minimal (Table II).

5. Conclusions

Exposure of the boron to the hydrogen plasma created boranes which were detected by SIMS analysis of the boron source after the deposition. The film deposition results indicated that boron was deposited from both ICP and CCP discharges over a range of H_2 concentrations, pressures and temperatures. The incorporation of oxygen in the film was thermodynamically favoured and dependent upon the substrate temperature. The H_2 plasma transport process can also transport other species in addition to B, including Si, which lead to impurities in the film. The relationship between the process parameters and the film thickness was complicated because of the CCP/ICP discharge transition was dependent on the gas concentration and pressure plus impurities generated by the discharge.

Acknowledgements

I would like to thank Mr. Tsutsumi for taking SEM micrographs of the film and Dr S. Lawson for taking SEM micrographs of the boron source. The authors would also like to acknowledge the Japan Science and Technology Agency and the National Institute for Inorganic Materials Center of Excellence for their financial support extended to J. Cross during the course of this investigation.

References

1. P. A. KEARNERY, J. M. SLAUGHTER, D. H. SHEN and C. M. FALCO, *J. Vac. Sci. Technol. A* **13** (1995) 78.
2. S. KOMATSU, T. YOSHIDA and K. AKASHI, *J. Mater. Sci. Lett.* **4** (1985) 51.
3. G. I. BABAT, *J. Inst. Elec. Engng Pt. III* (*Radio Commun. Engng*) **94** (1947) 27.
4. Y. HIKOSAKA, M. NAKMURA and H. SUGIA, *Jpn J. Appl. Phys.* **33** (1994) 2157.
5. "Handbook of Auger electron spectroscopy", edited by L. E. Davis (Physical Electronics, Inc., Eden Prairie, Minnesota, 1976).
6. "Handbook of X-ray photoelectron spectroscopy", edited by J. F. Moulder and J. Chastain (Physical Electronics, Inc., Eden Prairie, Minnesota, 1992).
7. JCPDS card #6-0297, International Center for Diffraction Data, Swarthmore, PA.
8. W. ZIMMERMAN III, A. M. MURPHY and C. FELDMAN, *Appl. Phys. Lett.* **10** (1979) 71.
9. T. M. BESSMAN, technical memorandum TM-5775, Oak Ridge National Laboratories, Oak Ridge, TN 1977.
10. G. ERICKSON, *Chemic Scripta* **8** (1975) 100.

Received 2 October 1995
and accepted 20 January 1997